White Paper

Accurate, reproducible, and standardized quantification

A. Hans Vija, PhD, Carl von Gall, MD, and Partha Ghosh, MD
Siemens Healthineers
Molecular Imaging Business Line

SIEMENS Healthineers

Table of contents

Introduction 3
Clinical applications 4
- Orthopedics 4
- Oncology 5

Traditional quantification 5
limitations of SPECT/CT quantification using a relative reference 7
Introducing xSPECT Quant™ 8
The benefits of xSPECT Quant: clinical case studies 11
- Case study 1 11
- Background Information 11
- Findings 11
- The benefits of xSPECT Quant 12
- Case study 2 12
- Background information 12
- Findings 13
- The benefits of xSPECT Quant 14

Absolute quantitative SPECT/CT for ^{177}Lu, ^{111}In, and ^{123}I 15
- ^{177}Lu-related applications 15
- ^{111}In-related applications 20
- Case study 3 21
- Background information 21
- Findings 21
- The benefits of xSPECT Quant 21
- ^{123}I-related applications 23

Conclusion 26
Author 27
References 28

Introduction

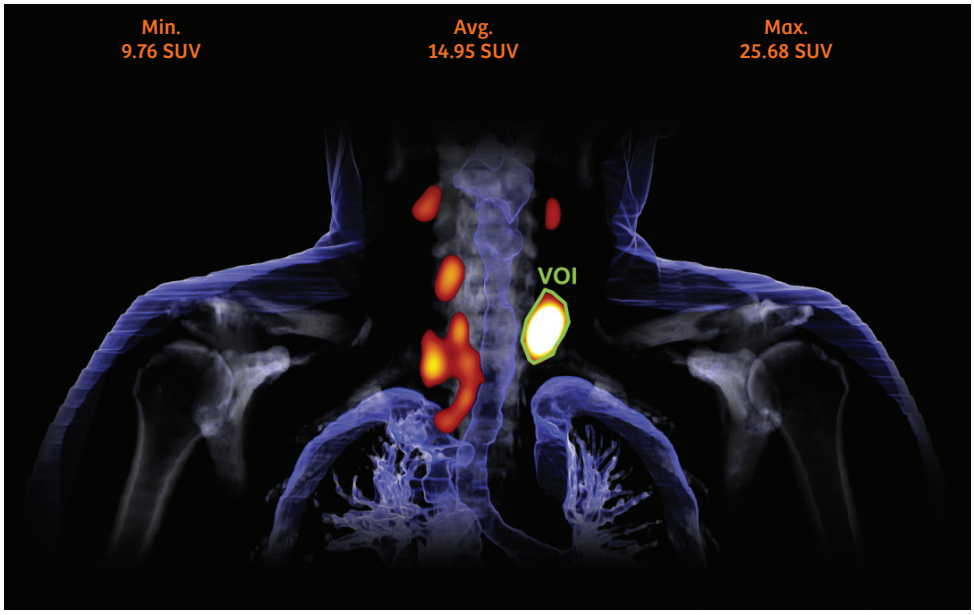

Figure 1: Clinical example of a patient scanned on a Symbia™ SPECT/CT system using xSPECT Quant. The image shows a ^{99m}Tc thyroid scan revealing a hyper-funtioning thyroid adenoma and the standard uptake values (SUVs) for defined volume of interest (VOI).

Data courtesy of
Friedrich Alexander University,
Erlangen, Germany.

Accurate and reproducible quantification has been a key objective since the early days of nuclear medicine. The ability to accurately quantify total radionuclide uptake in SPECT imaging has a number of increasingly important applications, such as theranostics.

However, there are a number of physical, patient, and technical factors that limit the quantitative reliability of nuclear medicine images.[1] Many traditional applications that involve quantification of nuclear medicine images use relative quantification only. This relative quantification involves ratios of image intensity values simply assuming that the effects of physical, patient, and technical factors like attenuation and scatter will cancel each other out. This is an erroneous assumption because the magnitudes of these factors are both spatially varying and patient-dependent.[2]

Absolute quantification addresses these limitations by accurately measuring the system physical characteristics as well as accurately incorporating the imaging physics.

One important benefit of using absolute quantification is standardization and consistency. Clinical applications, such as brain SPECT, require established benchmarks or thresholds often derived from normal databases; absolute quantification will ensure that reference values derived from databases are consistent across healthcare institutions, scanners, and time, and are independent of patient variability.

In June 2013, Siemens Healthineers Molecular Imaging (MI) introduced Symbia Intevo™ SPECT/CT and with it, xSPECT Quant, the first and only solution capable of delivering absolute quantification—paving the way for accurate, reproducible, and standardized quantitative clinical studies.

Clinical applications

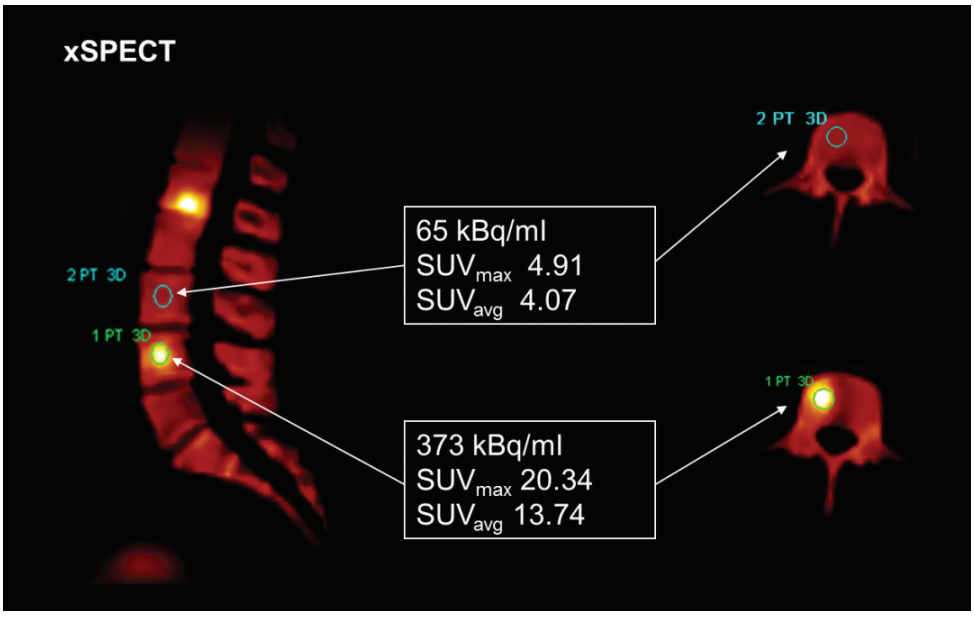

Figure 2: Lumbar vertebral metastases in a patient with lung cancer. xSPECT Quant confirms hot lesions are metastatic with high SUV but also uncovers zones with very low SUV in uninvolved vertebrae, suggesting osteoporosis.

Data courtesy of Johns Hopkins University, Baltimore, Maryland, USA.

There are several nuclear medicine applications that require images with absolute quantification accuracy.

Although SPECT imaging is a well-established modality, accurate and absolute quantification is only now gaining momentum. Therefore, therapy planning and treatment response evaluation has been a PET and PET/CT domain. With the advent of precise and robust quantification using xSPECT Quant, the quantitative domain in SPECT is becoming a reality in clinical practice.

Today, there are several clinical applications in nuclear medicine that benefit from accurate, reproducible, and standardized quantification.

Orthopedics

Osseous inflammation, such as osteomyelitis, often forces surgeons and orthopedists to perform secondary or even multiple surgeries, increasing patients' overall number of interventions and incident levels. The reporting of conventional SPECT images relies heavily on the visual interpretation and the expertise of the reading physician.

A quantitative approach using xSPECT Quant can help to differentiate a reactive focal increase in bone metabolism from significant uptake derived from inflammation. In a follow-up setting, reporting physicians can precisely inform referring clinicians of quantitative changes in the focal uptake and precisely monitor disease response to therapy. Shear stress related to joint pathology and prosthesis implantation defined quantitatively with xSPECT Quant may help in orthopedic decisions.

Oncology

Treatment of liver cancer and/or liver metastases from other cancers using nuclear medicine has become clinical routine.

For shunt volume measurement, the standard practice is to use ratios defining the relative fraction of tracer to pulmonary tissue and identifying possible shunts that may hamper therapy or even be hazardous to a patient's lungs.

A 3D quantitative approach like xSPECT Quant could replace the ratio standard practice with a more precise way of measuring the shunt fraction in each patient.

During or after therapy, xSPECT Quant is capable of accurate measurement of each of the lesion's responses. Initial values can be compared to follow-up scans and, using this quantification method, physicians can identify responders from non-responders, demonstrate clear changes to the referring clinicians, and give the patient an opportunity for treatment optimization.

Traditional quantification

The concept of quantification in nuclear medicine is not new.[1-5] We seek to estimate activity concentration of the radiopharmaceutical in Bq/ml *in-vivo*. Given the vast range of possible isotopes used in nuclear medicine, it is a very complex task that has eluded satisfactory solution in clinical practice. Quantitation is inherently a volumetric problem which requires tomography to solve it. The principle solution for quantification only became tractable once computing power was high enough to allow for iterative reconstruction with all the needed corrections to be performed in a clinical setting. The key requirement for reliable patient-specific attenuation correction (AC) was essentially solved with the advent of hybrid SPECT/CT systems with fast rotating and diagnostic quality CTs. Numerous publications have demonstrated the advantage of quantification, eg,[6-8], but there is no standardized approach.

The base unit in a gamma camera is the count. Traditionally, SPECT acquires, reconstructs, and delivers a 3D image in units of counts. A conversion method is then needed to compute Bq/ml, the simplest of which is to use a basic conversion factor post-reconstruction. Thus, by acquiring a test source for a known amount of time with SPECT, and then reconstructing that data with the method of choice, one can determine

Figure 3: Traditional method A calibrates the scanner using the dose calibrator as reference source.

1. Measure the total radionuclide activity in the syringe using a dose calibrator.

2. Insert tracer information, including the measured activity to the processing software workstation.

3. Perform a regular system scan using either a syringe or a dedicated phantom with the radionuclide dose of step 1.

4. Insert the system sensitivity in counts per second per unit of activity measured in step 3.

5. Set up the patient and perform the scan.

6. Provide patient information and compute estimated proportional counts per activity concentration based on steps 1–5.

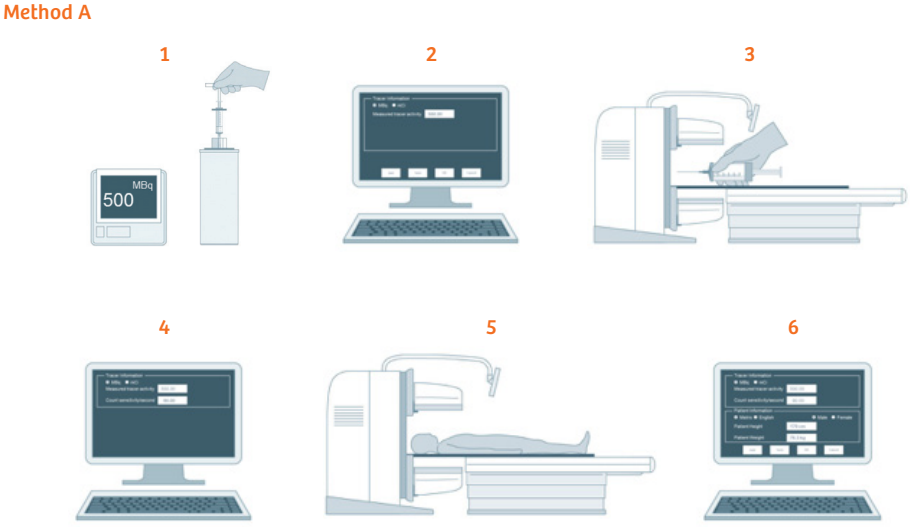

a conversion factor between the activity (in Bq) of the test source measured in the reference device (ie, dose calibrator) and the resulting counts in a 3D image of that test source. Once that conversion factor is obtained, one assumes that one can use the same conversion factor to convert data from a patient scan.

Ritt et al.[3] summarizes not only the basic steps needed to quantitatively measure the activity distribution, but also briefly describes common methods used to reconstruct and compensate for the various effects impacting the SPECT image formation. Zeintl et al.[4] describes a conversion method based on the dose calibrator as the reference device. The method essentially boils down to applying conversion factors from a list based on the volume sensitivity and the approporiate imaging condition (acqusition, collimators, counts, and reconstruction) and lesion size. Beauregard et al.[5] expands on the approach when focusing on a ^{177}Lu application at high count rates, and thus including a system dead time correction method. Please note that the conversion factors and dead time correction tables have to be measured on site and are only valid on that machine at that point in time.

Methods relying on the dose calibrator can only be as accurate and precise as the dose calibrator itself, in the sense that they may work well at a site under a certain protocol, but may be hard to translate to other sites and users yielding the same accuracy and precision.

Limitations of SPECT/CT quantification using a relative reference

Method B

Figure 4: Traditional method B calibrates each scan with a syringe.

1. Measure the total radionuclide activity in the syringe using a dose calibrator.
2. Insert tracer information including the measured activity to the processing software workstation.
3. Set up the patient and place the measured radioactive syringe from step 1 at the patient's feet. Perform the scan.
4. Provide patient information and compute estimated proportional counts per activity concentration based on steps 1–3.

Relative quantification is an important aspect in nuclear medicine imaging analysis. "Relative" could indicate a comparison of uptake in different regions of the body, such as a left and right kidney, using a ratio of uptake. Clearly, in this case the unit of the voxel being either count or Bq/ml is irrelevant. Another "relative" measure is SUV, where the activity in a region is normalized to the injected dose assuming that the dose in the background is in first approximation uniformly distributed. Although such measures are often referred to as "absolute," they are actually relative values.

In relative quantification, the bias in the dose calibrator is not relevant as long as one uses the same dose calibrator to determine the calibration factor and the injected dose, as the bias in the SUV will cancel out. Inherently, all these measures imply a relation to the calibration source used to do the count-to-Bq conversion and thus to the dose calibrator used to calibrate the calibration source. For such quantification with a relative reference, the variability of the dose calibrators does not really matter.

However, if we envision using the SPECT system to assess biological variability in a patient over time, or to compare a pool of patient populations with the same disease or to perform internal dosimetry estimations, one needs to have a reference standard that has small variability and allows for reliable measurement of absolute activity distribution *in-vivo*. Dose calibrators can have biases in excess of 10%[9], and should not be the reference standard when the goal is to achieve highly accurate absolute quantification.

Introducing xSPECT Quant

Siemens Healthineers MI introduced xSPECT Quant, setting the foundation for quantitative SPECT imaging. The goal was to create a National Institute of Standards and Technology (NIST)-traceable approach to deliver accurate and reproducible quantification of nuclear medicine tracers for such enabled SPECT systems.

We use a calibrated sensitivity source (CSS), traceable to NIST, as the gold standard. The intent of the CSS calibration is to standardize the system sensitivity, so that quantitative results can be compared across systems and time. Each CSS contains either a ^{57}Co (for low energy) or a ^{75}Se source (for medium energy) with an activity accurate to within a 3% [99% confidence level (CL) or 2.56σ] NIST-traceable uncertainty of the known manufactured strength, which itself resides within a 15% acceptance range of the nominal 111 MBq. Following proper SPECT calibration, the CSS should be extended once a month into the field of view (FOV) at a precise location to calibrate out system-specific sensitivity variation.[a] The xSPECT system is designed to estimate the activity concentration as an integral part of the reconstruction process and the result is an image in units of Bq/ml. No further conversion is needed. The CSS should also be placed in a dose calibrator within a holder that specifies the geometry and allows for a cross-check between the system, the dose calibrator, and the CSS.

Monthly activities:

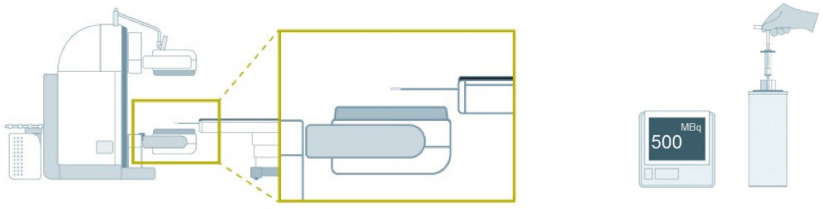

Per scan activities:

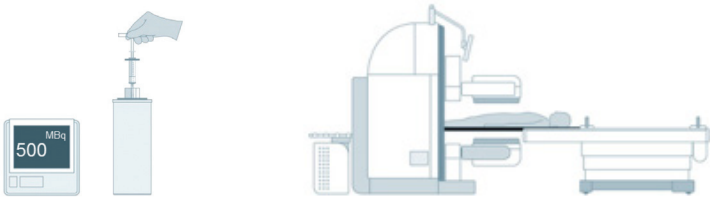

Figure 5a: xSPECT method calibrates the scanner and can be used to calibrate the dosimeter.

Description of xSPECT quantification workflow.

Monthly activities:
1. Calibrate the scanner once every month (12–20 minutes).

2. Can be used to calibrate the dosimeter.

The xSPECT™ method is described in detail in [10]. The key highlights include its ability to:

1. Measure system characteristics, either as a class standard or for an individual component ("fingerprint").
2. Perform iterative reconstruction using an additive update scheme using Mighell's modified X_γ^2 as the objective function and a pre-conditioned conjugate gradient as the minimizer.[11]
3. Ulitize data that is uncorrected and apply corrections in image space, where the reference coordinate system is the CT frame-of-reference.

The characterization of the image formation is anchored by the point spread function (PSF) as measured over the entire FOV and at different distances. For ^{99m}Tc and LEHR, about 90% of the counts are inside the purely geometric footprint (ie, the region without septal penetration).

In 2016, the quantitative xSPECT formalism was extended beyond ^{99m}Tc and LEHR for diagnostic use at a low count rate.

Monthly activities:

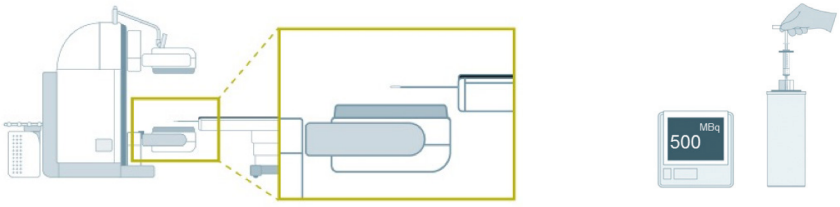

Per scan activities:

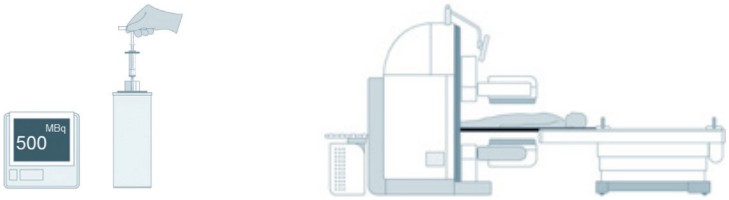

Figure 5b: xSPECT method calibrates the scanner and helps cross-check the dosimeter accuracy using the same calibrated source.

Description of xSPECT quantification workflow:

Per scan activities.

1. Measure the total radionuclide activity in the syringe in the calibrated dosimeter.
2. Scan the patient and retrieve automatic absolute quantification in your reconstruction console.

The same approach as used for ^{99m}Tc xSPECT Quant in 2013 was adapted for ^{99m}Tc and ^{123}I on the LPHR, and ^{111}In and ^{177}Lu on the MELP collimator. In addition, the user was given tools and flexibility to quantitatively acquire other isotope configurations.

The count rate can be very high in theranostic applications and, thus, the detector level processing was adapted to improve imaging at these high count rates. Most importantly, a proprietary patient-dependent real-time measurement of the count loss fraction was introduced. This information is then used in the reconstruction.

All compensations, conversions, and use of calibration data occur within the reconstruction, preserving the Poisson nature of the data, and in itself represents a paradigm shift from the traditional approach that attempts to "correct" projection data. xSPECT reconstructs the activity concentration in Bq/ml at injection time in the diagnostic use case. The resulting xSPECT reconstructed data can be used for internal dosimetry calculations.

EMI can also be incorporated in our additive update mechanism allowing for multi-modal reconstruction, such as xSPECT Bone™. An expansion of EMI-enabled clinical applications beyond bone imaging is currently in research, as well as improvement to corrections schemes to further reduce uncertainties in the measurement and improve image quality and fidelity.

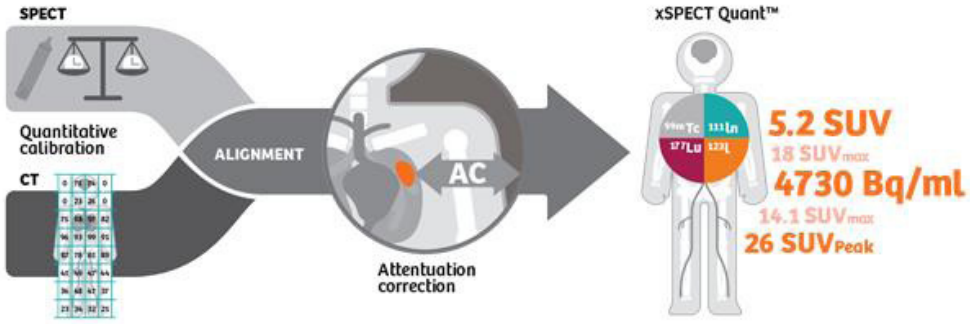

Figure 5c: Symbia Intevo with xSPECT Quant is the only nuclear medicine system capable of delivering absolute quantification that is both accurate and reproducible.

The benefits of xSPECT Quant: clinical case studies

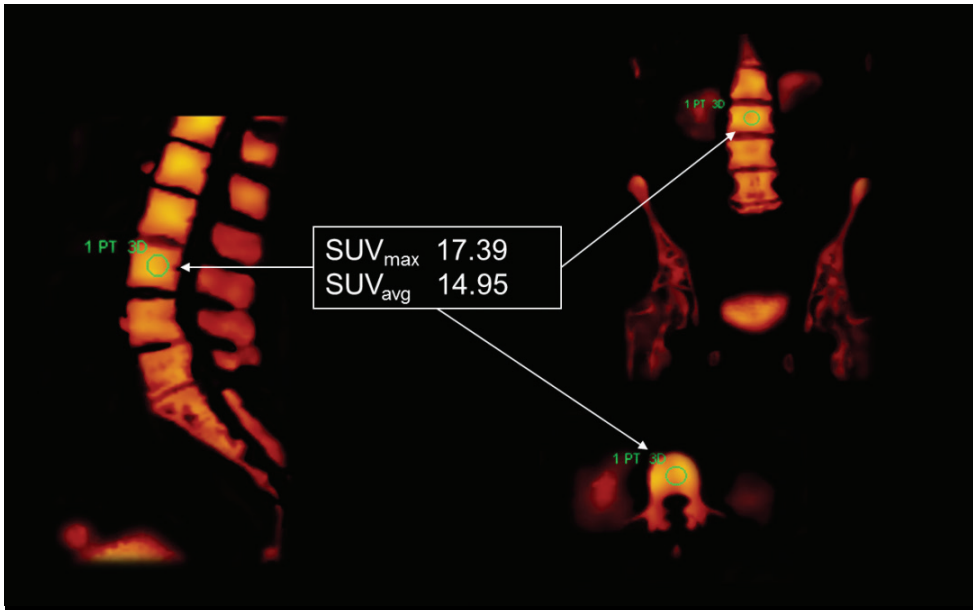

Figure 6: Diffuse vertebral metastases.

Data courtesy of University of Minnesota, Minneapolis, Minnesota, USA.

By establishing an accurate, reproducible, and standardized quantitative method with xSPECT Quant, the clinical utilities are extensive. Below are examples of where xSPECT Quant was able to impact the clinical decision-making process.

Case study 1
Background information

A 70-year-old woman with a history of breast carcinoma treated with surgery and chemotherapy underwent ^{99m}Tc MDP bone scintigraphy for routine follow-up. The planar study was followed by a SPECT/CT study of the lumbar spine performed on a Symbia T2 scanner.

Findings

The planar whole-body scan showed normal tracer uptake throughout the spine, except for degenerative changes in lumbar vertebrae. xSPECT showed uniform distribution of the tracer throughout the lumbar vertebrae with increased uptake in the right facet joint in L5 vertebrae secondary to facet arthropathy, as well as clear and sharp delineation of lamina, spinous process, and spinal canal. Visual evaluation of the CT and fused (CT +xSPECT Bone) images, however, shows a different clinical picture. CT shows diffuse sclerosis involving all the lumbar vertebrae including the body of the sacrum and the lamina and spinous processes. Such diffuse sclerosis could potentially reflect diffuse osseous metastases. Visually, the ^{99m}Tc MDP uptake in the sclerotic vertebrae appears uniform without any focal increase. Visualization of kidneys and bladder activity exclude a superscan appearance.

The benefits of xSPECT Quant

Using xSPECT Quant, the tracer concentration in kBq/ml could be obtained and, using injected dose and patient height and weight information, the SUV of individual voxels as well as volumes could be calculated.

Absolute quantification of tracer concentration in the lumbar with xSPECT Quant shows SUV_{avg} of 14.95 in the center of the body of L3 vertebrae (arrow), which is more than 2 times higher than that of normal (SUV_{avg} of 5.91). This high SUV within the lumbar vertebrae along with the diffuse sclerosis on CT is reflective of diffuse osseous metastases. However, the planar bone study did not show diffuse vertebral hypermetabolism and both kidneys were visualized, excluding a "superscan" appearance. This can be explained by the response of the diffuse vertebral metastases to chemotherapy, but with a persistently higher level of vertebral metabolism due to the increased bone turnover within the sclerotic component, as evident in the increased tracer concentration and SUV within the vertebrae.

Quantitative measurements in lumbar vertebrae of 50 normal female patients yielded an average bone tracer activity concentration of 48.15 ± 13.66 kBq/ml, which corresponded to SUV_{avg} of 5.91 ± 1.54.[12]

Case study 2
Background information

A 74-year-old female with open comminuted fracture of upper part of left tibia was treated with surgical reduction of fracture and internal fixation with flap reconstruction surgery for the surface wound. The tibial plateau fracture was treated with internal fixation using a dual plate. Subsequent to the surgery, the patient experienced persistent pain, wound discharge and non-union of the fracture fragments. In view of the suspicion of osteomyelitis of the tibial fracture fragments, the patient underwent infection imaging with ^{99m}Tc-labelled antigranulocyte antibodies and SPECT/CT. The study was performed on a Symbia Intevo scanner.

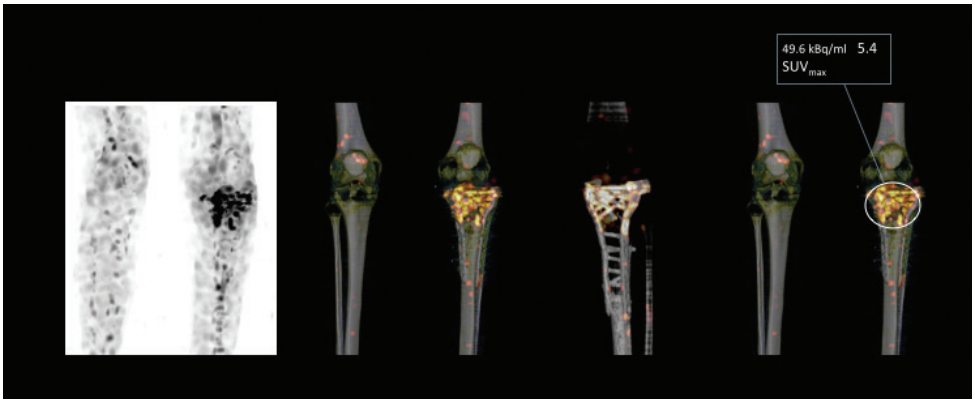

Figure 7: Pre-surgery SPECT/CT imaging of infection in tibial fracture with internal fixation with ^{99m}Tc antigranulocyte antibody* with xSPECT Quant evaluation of SUV of leucoctye accumulation.

Data courtesy of University of Bundeswehrkrankenhaus, Ulm, Germany.

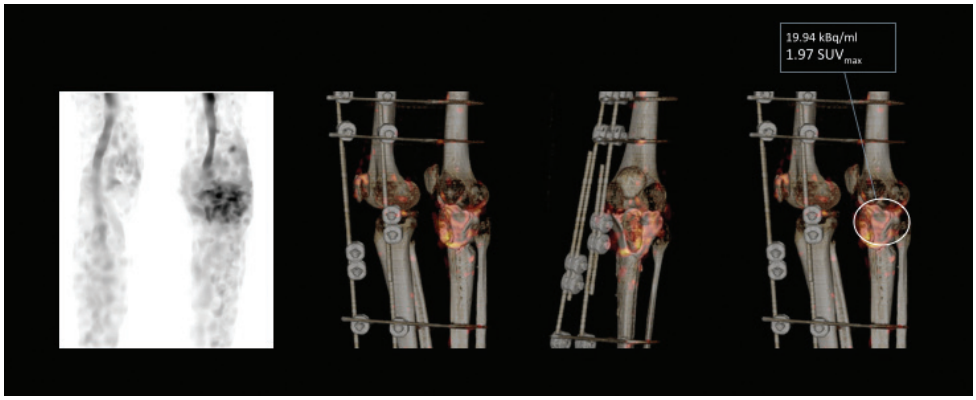

Figure 8: Post-surgery follow-up SPECT/CT infection imaging with ^{99m}Tc antigranulocyte antibodies with SUV quantification using xSPECT Quant.

Data courtesy of Bundeswehrkrankenhaus, Ulm, Germany.

Findings

SPECT/CT acquisition was performed 5 and 24 hours following injection with absolute quantification of tracer uptake. Absolute quantification and SUV_{max} values were obtained using xSPECT Quant and compared across 5- and 24-hour acquisitions. SPECT/CT images show focal areas of intense inhomogeneous accumulation of ^{99m}Tc-labelled antigranulocyte antibodies within the fracture fragments in the proximal end of left tibia as well as the internal fixation plates, especially the intercondylar plate. The pattern of uptake is suggestive of active osteomyelitis. SUV_{max} comparisons showed a significant increase between the 5- and 24-hour acquisitions in all areas of focal uptake (SUV_{max} increase from 2.61 to 4.55 in one foci shown in Figure 7) suggestive of progressive accumulation of radiolabelled antigranulocyte antibodies, which reflect progressive leucocyte accumulation within the infective foci involving the fracture fragments and internal fixation pins and plates of the proximal tibia, suggestive of active osteomyelitis.

In view of the extent of active osteomyelitis, the patient underwent a revision arthroplasty with complete removal of all metal internal fixation plates, resection of the majority of the proximal tibia including the condyles, and replacement of the proximal tibia with gentamicin impregnated bone cement spacer along with external fixation of the femoral and tibial shafts. A delayed arthrodesis, once the bone is free from infection, was planned. Microbiological evaluation of the resected tibial bone fragment demonstrated Propionibacterium acnes infection.

Two months after surgery, the patient underwent SPECT/CT imaging for evaluation of the presence of infection using ^{99m}Tc-labelled antigranulocyte antibodies (Leukoscan) to assess the feasibility of arthrodesis. A similar protocol of SPECT/CT acquisition at 5- and 24- hours after tracer injection was followed with SUV comparison using xSPECT Quant.

CT shows a radiodense mass at the proximal end of the tibia which reflects the cement spacer inserted following resection of the majority of tibial head. The cement fits between the femoral articular surface and the upper end of the tibial shaft. The junction of cement spacer and tibial shaft is irregular, suggesting pseudoarthrosis.

The external fixation devices are well-delineated. Fused images show a small area of mildly increased uptake at the junction of the dense cement spacer and the tibial shaft reflecting mild accumulation of leukocytes secondary to reactive changes which are secondary to pseudoarthrosis at the bone cement junction. SUV_{max} in the junction between the radiodense cement spacer and the shaft of the tibia was 1.31 in the 5-hour study but increased only slightly to 1.82 in the 24-hour study. This very mild increase in an extended time period suggested the absence of active infection which is usually associated with much higher leucocyte migration and accumulation in infected bone.

The benefits of xSPECT Quant

SUV_{max} estimation using xSPECT Quant thus provided an objective measurement to evaluate granulocyte migration inside the suspected foci. Moreover, the initial SUV_{max} of 1.31 was also very low, and corresponded to the visual impression of only mild uptake, which reflects reactive changes at the level of pseudoarthrosis.

As evident from Figure 9, xSPECT Quant measurements of bone metabolism in the rib and scapular lesions before and three and eight months after initiation of therapy with androgen synthesis inhibitor shows declines in lesion SUV which correlate with serum PSA decline although the SUV decline slightly lags behind the drop in PSA. This shows a dramatic reduction in the first three months of therapy. Although visually the rib lesion showed only a minor decrease in uptake after three months, the decline in SUV from 24.3 to 16.8 was more than anticipated from the visual evaluation. The sclerosis in the rib lesion also progressed as seen on CT with a progressive decrease in tracer uptake reflecting therapy response.

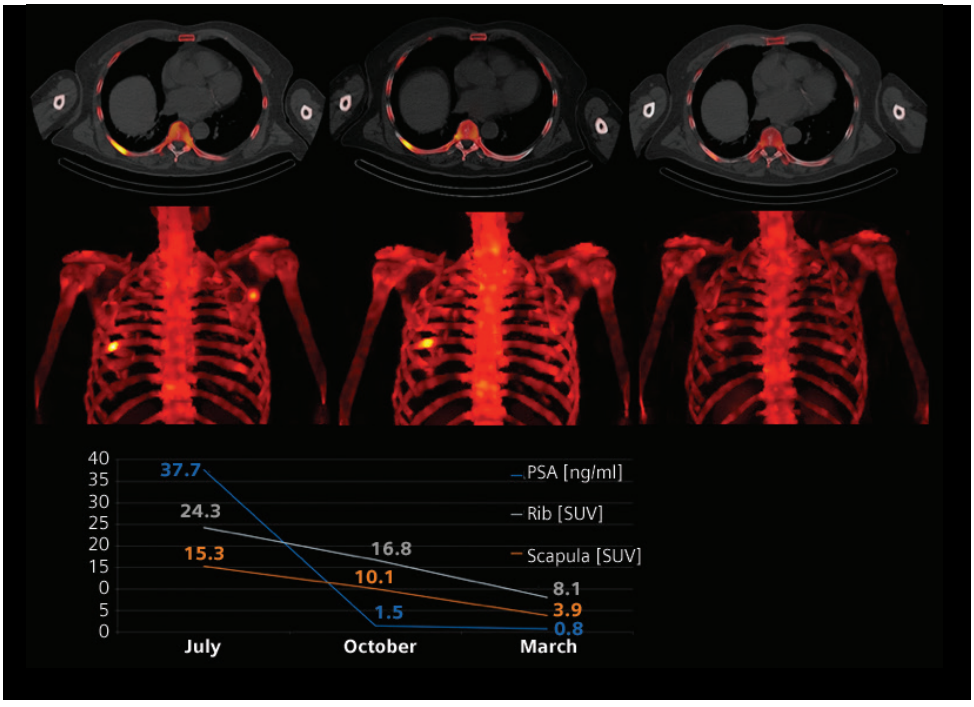

Figure 9: Sequential ^{99m}Tc-MDP SPECT/CT in a patient with osseous metastatic prostate cancer and elevated prostate-specific antigen (PSA) enrolled in treatment initialization with an androgen synthesis inhibitor. Pre-therapy xSPECT Bone shows hypermetabolic rib and contralateral scapular lesion. Three months after treatment, by visual analysis, a significant decline in tracer uptake for the scapula but only barely reduced uptake in the rib was found. The next study performed eight months after treatment onset shows a significant decrease in rib lesion and near normalization of scapular lesion. xSPECT Quant evaluation by SUV of the rib and the scapular lesion, as depicted in the graph, showed a significant decline for both lesions after three months already. In addition, the decline of SUV corresponded well with decline of serum PSA, shown in the graph as well.

Data courtesy of CHRU de Brest, Brest, France.

Absolute quantitative SPECT/CT for ^{177}Lu, ^{111}In, and ^{123}I

Absolute quantification with SPECT/CT has expanded from initial application for ^{99m}Tc-labelled radiopharmaceuticals to other isotopes like Lutetium-177 (^{177}Lu), Indium-111 (^{111}In), and Iodine-123 (^{123}I). Expansion of reproducible quantification of absolute tracer concentration using SPECT/CT for radiopharmaceuticals labelled with these isotopes has major implications in diagnosis and management of a spectrum of diseases, such as neuroendocrine tumors. Absolute quantification with SPECT/CT could potentially be helpful in assessment of disease burden, improvement in dosimetry evaluation, and evaluation of therapy response in tumors such as metastatic carcinoid, neuroblastoma, and pheochromocytoma. Recently introduced radionuclide therapies like ^{177}Lu-labelled PSMA for treatment of metastatic prostate cancer may be significantly impacted by use of sequential quantitative SPECT/CT for evaluation of radiation dose to tumor and critical organs like kidneys and bone marrow, as well as accurate estimation of response and prediction of feasibility of multiple therapy administrations.

^{177}Lu-related applications

Substantial literature exists to support the routine use of quantitative SPECT/CT for initial evaluation and dosimetric assessment for neuroendocrine tumors (NETs). Most NETs express somatostatin receptors, in particular SST2 receptors which results in high uptake of radiolabeled somatostatin analogs like ^{177}Lu-DOTATATE which is being increasingly used for treatment of patients with advanced metastatic NETs with peptide receptor radionuclide therapy (PRRT). Apart from β emission, ^{177}Lu-DOTATATE is also a gamma emitter which allows planar and SPECT imaging to be performed following therapeutic dose, enabling demonstration of tumor uptake and estimation of tumor and critical organ dose along with prediction of therapeutic efficacy and need and feasibility of multiple therapies. ^{177}Lu has a half-life of 6.7 hours, a beta tissue penetration of 2 mm, and main gamma photopeak of 208 keV (10.4% probability) with 113 keV (6.4%) being the other photopeak.

Following radionuclide therapy with ^{177}Lu-DOTATATE in NETs, complete response is seen in less than 5%, partial response in 10-35% while the bulk of patients (50–80%) have stable disease.[13] Ten to 20 percent of patients, however, show progressive disease in spite of PRRT. The standard therapy approach with ^{177}Lu-DOTATATE is for 4 cycles to be administered at 8-11 week intervals with each therapy dose being 7–7.4 GBq. More cycles are added based on tumor and critical organ dosimetry, and toxicity to bone marrow and kidney evaluated by serial platelet counts and serum creatinine, and creatinine clearance. Cumulative bone marrow and renal dose are the limiting factors concerning the number of therapy cycles and total dose delivered.

In view of the low levels of complete or partial response following radionuclide therapy, a fundamental objective of quantitative SPECT/CT is to improve dose estimations to critical organs to optimize radionuclide therapy dose administration to achieve highest tumor dose while limiting potential toxicity.

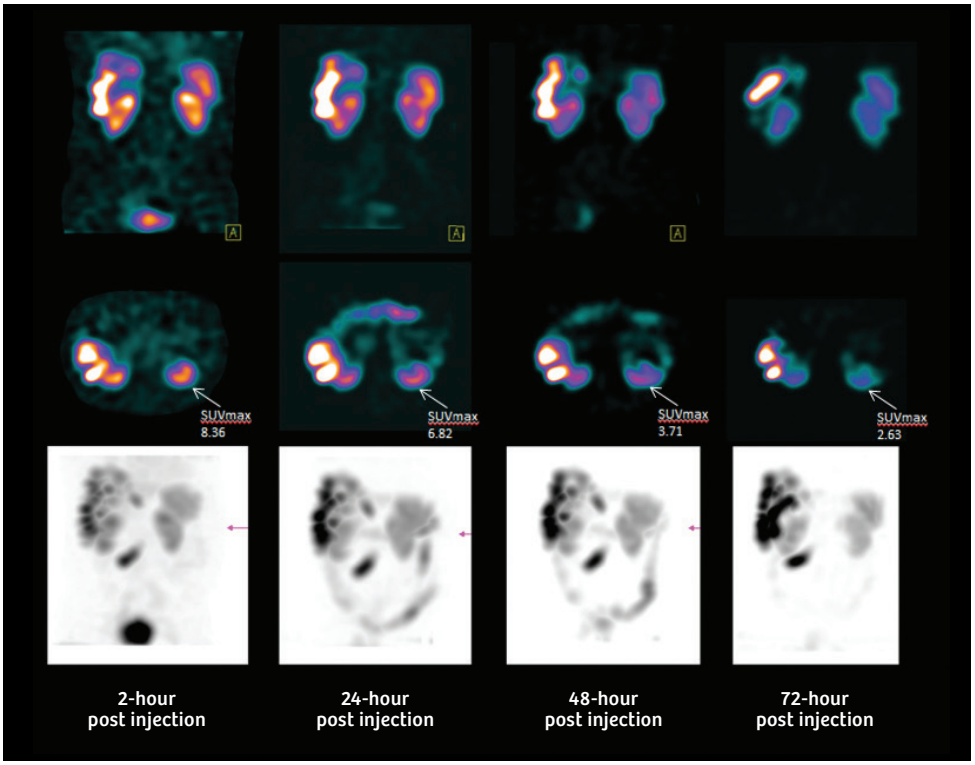

Figure 10: Sequential quantitative SPECT/CT over four time points following therapeutic dose of ^{177}Lu-DOTATATE in a patient with metastatic NET.

Data courtesy of Ludwig Maximilians University, Munich, Germany.

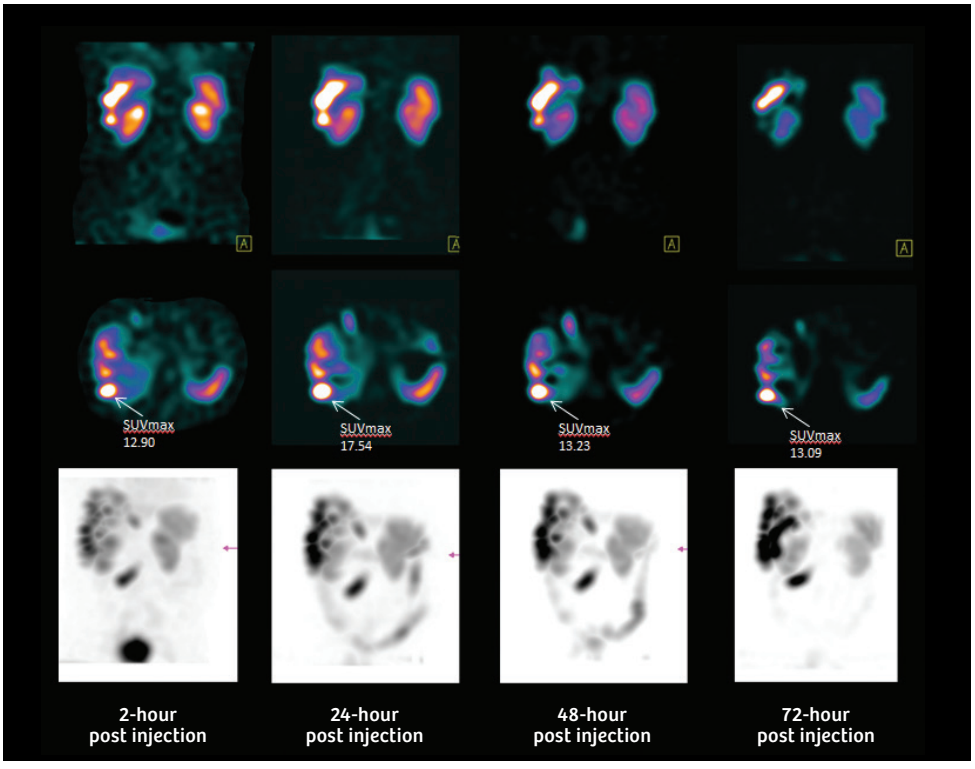

Figure 11: Sequential quantitative evaluation of liver metastases showing changes in SUV_{max} across four time points. SUV_{max} of metastases in right lower part of liver (arrow) is calculated as 12.90 at 2 hours after tracer administration. There is a significant increase of SUV_{max} to 17.54 at 24 hours reflecting progressive tumor absorption of radiolabeled ^{177}Lu-DOTATATE. SUV_{max} decreases subsequently to 13.23 at 48 hours. Tumor uptake remains similar between 48 and 72 hours (13.09). The SUV estimation of individual lesions helps determine total tumor tracer concentration and clearance enabling assessment of total tumor dose.

Data courtesy of Ludwig Maximilians University, Munich, Germany.

Figure 10 shows sequential quantitative SPECT/CT acquisition in a patient with multiple liver metastases from neuroendocrine tumor acquired 2, 24, 48, and 72 hours after therapeutic administration of 7 GBq of ^{177}Lu-DOTATATE. Visual evaluation of MIP SPECT images (bottom row) shows multiple tracer-avid liver metastases, which indicate an increase in uptake between 2 and 24 hours with relatively stable tumor uptake from 24 to 72 hours. The renal uptake appears to gradually decrease on visual inspection from 2 hours to 72 hours. Quantitative SPECT/CT enables SUV estimation of lesions and critical organs such as the kidney across multiple time points. SUV_{max} measurements of the left kidney across all four time points (middle row) show initial (2-hour) SUV_{max} of 7.05, which decreases to 6.32 at 24 hours with a further decrease to 4.71 at 48 hours and 3.34 at 72 hours. Kidney uptake thus shows a continuous gradual clearance as quantitatively evaluated. A considerable amount of tracer clearance into the colon is visualized from the 24-hour time point to the 72-hour time point. Estimation of total tracer concentration in the renal cortex across multiple time point studies enables accurate estimation of tracer retention and transit leading to proper estimation of renal dose following therapy, as well as prediction of cumulative renal dose.

Renal toxicity has been reported in about 35% of patients treated with PRRT, however, only 1.5% had grade 3–4 toxicity which involves a rise in serum creatinine three times above baseline levels.[14] Hypertension, diabetes, and previous chemotherapy have been known to increase the risk of renal damage following PRRT. Although concomitant amino acid infusion reduces the renal toxicity during PRRT, strict adherence to the practice of limiting cumulative renal dose to 23 Gy or less is currently the accepted approach to ensuring absence of significant renal toxicity during PRRT.

Bone marrow toxicity following PRRT is commonly associated with transient thrombocytopenia, anemia, and reduction in leucocyte counts. Only 10% of patients show grade 3 or 4 toxicity. Bone marrow toxicity is rare with ^{177}Lu probably due to the shorter beta tissue travel as compared to ^{90}Y which has 12 mm beta tissue penetration. A cumulative bone marrow dose limit of 2 Gy is widely adopted as a guideline for PRRT planning.

In a study involving 310 patients treated with 4 cycles of ^{177}Lu-DOTATATE therapy, 29% had partial response, 16% had minor response with 25–50% reduction in tumor volume, and 35% had stable disease when evaluated 3 months after delivery of last therapy cycle.[15] Median overall survival was 46 months while median progression-free survival was 33 months. Extent of liver involvement was a key predictor of overall survival. Subacute grade 3 or 4 hematological toxicity, predominantly thrombocytopenia, was seen only after 3.6% of administrations and was associated with lower creatinine clearance, presence of bone metastases, and history of previous chemotherapy.

In PRRT, the therapeutic objective is to administer the highest amount without exceeding the maximum radiation dose limit of organs at risk, such as kidney and bone marrow, to achieve the maximum tumor dose without undue risk of toxicity. The number of therapies thus depends on the cumulative absorbed dose to the kidneys and bone marrow which can be evaluated using sequential planar or SPECT imaging and subsequent dosimetric evaluation of data. The maximum accepted doses are 23 Gy to the kidneys and 2 Gy to the bone marrow. In view of the potential impact of renal and bone marrow toxicity on the decision of the number of therapies of ^{177}Lu PRRT, the accuracy of dosimetry for assessment of the radiation dose to the kidneys and bone marrow is critical to therapeutic efficacy and outcome. Sequential whole body planar scintigraphic acquisition following administration of therapeutic dose of ^{177}Lu-DOTATATE has been used for tumor and organ dose estimation by several sites. However, sequential SPECT/CT-based dose estimations have been proven to improve accuracy, especially for renal dose since proper separation of kidney from the liver and adjacent tumor, and abdominal uptake is often difficult using a planar study.

Comparison of whole-body planar scintigraphy-based and sequential quantitative SPECT/CT-based dosimetry estimations in patients treated with ^{177}Lu-DOTATATE have shown that dosimetry using the planar method leads to higher absorbed dose calculations in most patients.[16] This study evaluated 21 patients with disseminated NET who were treated with ^{177}Lu-DOTATATE with sequential whole-body planar studies performed immediately after tracer administration and at 24, 96, and 168 hours. SPECT/CT was performed in every patient at 24 and 96 hours following tracer administration. Dose to kidneys was calculated using 3 different methods: whole-body planar-based dosimetry, dosimetry based on planar studies, including one SPECT data used to scale the amplitude of the time activity curve obtained from planar images, and a SPECT/CT-based method where absorbed dose rates were calculated using a volume of interest defined over the renal cortex on the attenuation corrected quantitative SPECT images. Median absorbed dose to the kidneys cumulated across all therapy cycles calculated using planar method was 26 Gy (range 17–45 Gy) while the corresponding value obtained with quantitative SPECT/CT was 21 Gy (range 14–32 Gy). The major cause for such a higher renal dose estimation using the planar-based method was the overlap of high intestinal and liver activity with the renal activity, which led to overestimation of the kidney activity. Based on planar-based dosimetry, 7 out of 21 patients received an absorbed dose to the kidney which exceeded the maximum tolerated renal absorbed dose accepted by the authors at 27 Gy. Thus, overestimation of dose on planar-based dosimetry may lead to patients being undertreated to avoid excessive renal dose. This study illustrates clearly the need for quantitative SPECT/CT-based dosimetry with increased accuracy for renal dose estimations in order to avoid undertreatment.

Nephrotoxicity with ^{177}Lu-DOTATATE therapy has been estimated to be low with average annual decrease in creatinine clearance of 3%.[17] Amino acid infusion during PRRT has been shown to further reduce renal toxicity. In a large series of 323 patients treated with PRRT, none of the patients had an annual decrease in renal function of more than 20% with the mean radiation dose to the kidneys being 20.1 +/- 4.9 Gy.[18] In patients with large tumor burden with high receptor density, sequestration of radiotracer within the tumor may lead to reduced bioavailability to kidneys and bone marrow, thereby further decreasing the absorbed dose to critical organs (tumor sink effect).[19] The 23 Gy limit for cumulative renal dose is based on the absorbed dose limit used in external beam radiotherapy and may not be appropriate considering the lower dose rate of PRRT. Higher absorbed dose limits to the kidney up to a limit of 29 Gy have been advocated.[20] The possibility of increasing therapeutic dose and number of therapies depending on individual patient tumor burden and tumor and critical organ dose estimation is a key factor driving adoption of PRRT. Quantitative SPECT/CT with accurate and reproducible estimation of absolute tracer concentration within tumor and critical organs promises to further improve the accuracy of dosimetric estimation which may avoid over and undertreatment of patients taking into account the biokinetics of radionuclide transit in the individual patient.

Radionuclide therapy of NET has been associated with large intrapatient and intralesional variability in tumor uptake and response. Tumor absorbed dose using ^{177}Lu-DOTATATE PRRT has been shown to correlate significantly with tumor response.[21] In this study involving 24 lesions, the tumor response varied from 4.5–57% and absorbed doses after 4 to 6 cycles were between 20 and 340 Gy. The majority of lesions achieved 10–30% reduction following PRRT. The majority of tumors achieved best response after 40–80 Gy while the tumors with the maximum percentage (>40%) decrease in volume received higher than 200 Gy. Some lesions received a higher absorbed dose but showed only minor reduction in size, which may be related to factors like hypoxia, necrosis, and

proliferation rate. In view of the variability of tumor response when exposed to similar levels of absorbed doses, it is essential to achieve the highest accuracy of tumor and critical organ dose estimations in order to better predict therapy efficacy and prescribe number of therapies in order to achieve sufficient therapeutic dose without compromising critical organ function. Reduction of partial volume effects appears to be a key driver of improved accuracy of dose estimation since this study clearly showed a better correlation of best response percentage tumor shrinkage and absorbed dose in lesions larger than 4 cm.

Sandstrom et al.[22] performed dose estimation of kidney and bone marrow using sequential planar and SPECT/CT following ^{177}Lu-DOTATATE therapy on 200 patients with metastatic NET. Anterior and posterior planar and SPECT/CT studies were performed at 24, 96, and 168 hours after administration of a therapeutic dose of 7.4 GBq of ^{177}Lu-DOTATATE. Blood samples were drawn for bone marrow dose estimation as well. Time activity curves were generated from activity concentrations measured within volumes of interest generated in kidney, normal liver, and spleen in the SPECT/CT studies. Whole-body planar images and blood activity concentrations were used for bone marrow dose estimation. Absorbed dose to kidneys ranged from 2–10 Gy per therapy cycle while that for bone marrow ranged from 40 to 225 mGy. Mean cumulative renal dose was approximately 9 Gy for all therapy cycles. Dose limiting organ was the kidney in 98.5% and the bone marrow in only 1.5% of the patients. Kidney and bone marrow dose was lower in subsequent therapies compared to the first therapy. Kidney dose decreased by a median of 39% between first and third therapies. With a 23 Gy limit to the kidneys, 50% of the patients could receive more than 4 cycles of therapy. However, dosimetry studies concluded that 20% patients could tolerate less than 4 therapy cycles without crossing renal dose limits. Such a possibility of undertreating patients based on dosimetric estimations of renal and marrow dose, the progressive lowering of renal dose in subsequent therapies, and the overall low incidence of renal toxicity opens up the possibility of improved selection of patients for further therapies based on more accurate dosimetry studies made possible by improved quantitative SPECT/CT accuracy.

Bailey et al.[23] performed a similar study using quantitative SPECT/CT at 0.5, 4, 24, and 96 hours after no-carrier added ^{177}Lu-DOTATATE administration in 13 patients with metastatic NET, each receiving 3 cycles with average dose of 7.8 GBq per cycle. Time activity curves generated from sequential SPECT/CT images with estimation of absolute tracer concentration enabled determination of absorbed dose to the kidneys using a bi-exponential fit which yielded a mean renal dose of 3.1 +/- 1.0 Gy per cycle (range 1.1–5.4 Gy) or 0.40 +/- 0.13 mGy/MBq. The average renal dose in this study was substantially lower than that estimated by Sandstrom et al. in the study mentioned previously[22] although both patient populations were similar with similar initial therapy doses as well as amino acid infusion protocols. The higher number of sequential SPECT/CT studies by Bailey et al., possibly leading to fitting to a multi-exponential clearance curve which could better characterize the tracer clearance pattern as compared to a mono-exponential curve, may be a possible explanation for such a significant decrease in calculated renal dose.

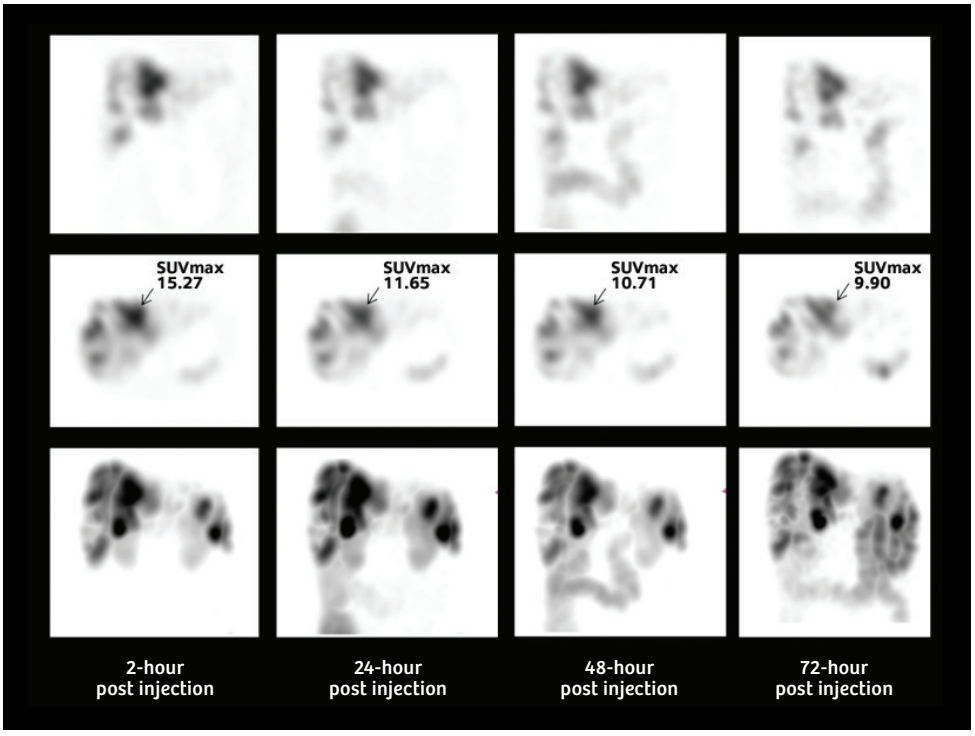

Figure 12: Sequential quantitative SPECT/CT in another patient with NET with multiple liver metastases treated with ^{177}Lu-DOTATATE showing high initial tumor SUV with gradual decrease over subsequent 3 time points. Note the progressive increase in tracer clearance through the colon.

Data courtesy of Ludwig Maximilians University, Munich, Germany.

^{111}In-related applications

Quantitative SPECT/CT is important for radiopharmaceuticals like ^{111}In-octreotide which is widely used for imaging of neuroendocrine tumors both for initial staging and for follow up after ^{90}Y-DOTATOC or ^{177}Lu-DOTATATE therapy. Quantitative approaches to determination of absolute tracer concentration and SUV using SPECT/CT have been performed for ^{111}In-octreotide. Rowe et al.[24] used phantom-based calibration methods to determine radionuclide uptake (SPECT-UV) for the kidneys and liver in 9 patients without obvious disease who underwent ^{111}In-octreotide SPECT/CT. Average SUV for the right kidney was 8.0 +/- 2.4 while that for the left kidney was 7.5 +/- 1.7. Liver SPECT-UV (1.7 +/- 0.6) was much lower than that of the kidneys.

The researcher analyzed the coefficient of variations (CV) of the liver, and the left and right kidney, as well. The left kidney demonstrated very low CV. Therefore, Rowe et al. recommended using the left kidney as an internal calibration to facilitate inter- as well as intra-individual changes in the uptake values.

Case study 3
Background information

Figure 13 shows sequential SPECT/CT study 2 and 24 hours following injection of 182 MBq of ^{111}In-octreotide in a 74-year-old man with history of primary NETs.

Findings

MIP images at 2 hours show physiological uptake in the kidneys, spleen, and liver without any well-defined focal uptake, suggestive of metastases. The 24-hour image shows slight increase in uptake in bilateral renal cortex as well as the spleen while liver uptake appears unchanged. Considerable bowel uptake is also visualized in the 24 hour image. xSPECT Quant study shows SUV_{max} and SUV_{peak} values in the kidneys, liver, and spleen. SUV_{max} at 2 hours in the renal cortex using ROI encompassing the whole of right kidney was 16.49, which increased to 20.16 at 24 hours. A spherical ROI in liver and spleen were used to calculate SUV. Splenic SUV_{max} was 22.55 increasing to 26.47 at 24 hours. Liver SUV was much lower (SUV_{max} 2.89 at 2 hours) increasing to 4.60 at 24 hours. This gradual increase in uptake in bilateral renal cortex, spleen, and liver, to a minor extent, is related to gradual clearance of circulating tracer into these organs in absence of tracer-avid tumor.

The benefits of xSPECT Quant

xSPECT Quant makes accurate and reproducible SUV estimation possible as demonstrated by the example in Figure 13 which enables reliable evaluation of tracer transit into and from tumor and critical organs. Accurate estimate of normal SUV range is key to evaluation of renal tracer transit and uptake levels in patients to assess cumulative renal dose accurately for radionuclide therapy with ^{177}Lu-DOTATATE or ^{90}Y-DOTATOC.

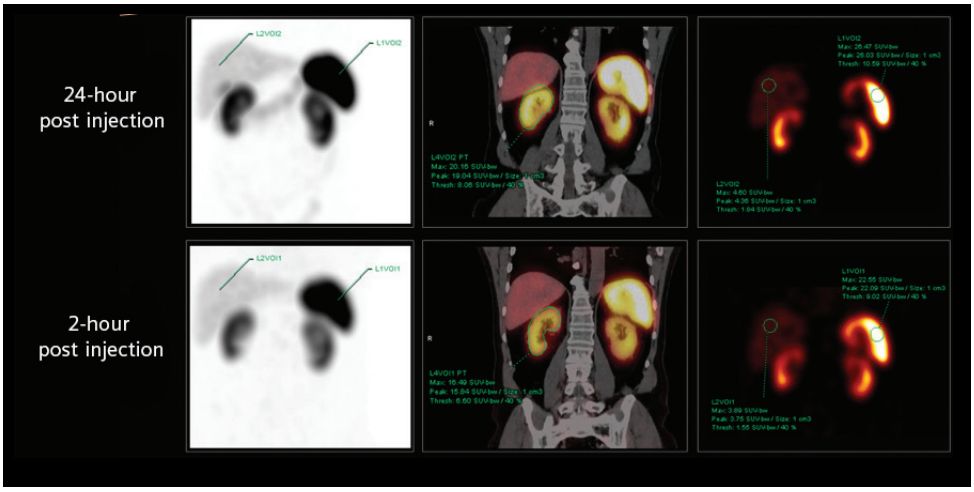

Figure 13: Sequential quantitative ^{111}In-octreotide SPECT/CT studies in a NET patient without metastases showing gradual increase in renal and splenic uptake activity over the course of 24 hours.

Data courtesy of CHUV, Lausanne, Switzerland.

Figure 14 shows an example of sequential ^{111}In-octreotide SPECT/CT in a patient with multiple liver metastases that show high tumor uptake with slow and gradual washout, thus indicating this patient to be an ideal candidate for ^{177}Lu-DOTATATE therapy. It is interesting to note that the renal SUV_{max} (10.05) at 2 hours is substantially lower than that of the patient in Figure 13 without any metastases (SUV_{max} of 14.86). The renal SUV_{max} in the metastatic patient progressively decreases to 6.74 at 24 hours while the renal SUV_{max} in the normal patient increases to 20.15 at 24 hours. The relatively low initial renal cortical SUV_{max} in the patient with extensive liver metastases may reflect the tumor sink effect since a large part of the injected radionuclide has been taken up by the tumor, leaving lower amount of circulating radionuclide to be excreted by kidneys. In the presence of normal renal function, there is gradual washout of the cortical tracer uptake at 24 hours. This is contrary to the situation in the normal patient where the renal uptake increases during the first 24 hours due to the high amount of circulating radionuclide due to absence of tracer-avid tumor.

Sequential scintigraphy after administration of ^{111}In-octreotide has been used to predict dose to tumor as well as liver and kidneys following ^{90}Y-DOTATOC therapy. Since ^{90}Y is a pure beta emitter, dosimetry requires imaging with ^{111}In-octreotide which closely mimics the uptake and clearance pattern of ^{90}Y-DOTATOC. Helisch et al.[25] performed whole-body planar imaging in 8 patients with metastatic NET immediately and 1, 4, 24, 30, and 48 hours after administration of 150–170 MBq of ^{111}In-pentetreotide using medium-energy general purpose parallel-hole collimator acquiring both 171 keV and 245 keV photopeaks. Additional SPECT studies were acquired 5 and 25 hours post-injection to improve the separation of tumor from adjacent liver and kidneys for more accurate ROI delineation. Time activity curves generated from sequential ^{111}In-octreotide scintigraphy were used to calculate predicted dose following ^{90}Y-DOTATOC therapy (4.44 GBq per cycle, 3 cycles each). Cumulative dose to the spleen was calculated to be the highest (3.31 +/- 1.02 mGy/MBq) followed by the kidneys (1.98 +/- 0.75 mGy/MBq). Estimated total radiation burden to the kidneys varied between 7.5 Gy to 36.9 Gy for therapy with 13.32 GBq of ^{90}Y-DOTATOC. Since the calculated renal dose exceeded the threshold of 27 Gy, 2 patients were excluded from radionuclide therapy. This study also demonstrated the limitations of planar-only imaging for dosimetry since in two patients the kidney and liver could not be separated on planar images to properly draw ROIs. Intense bowel activity was also a problem which could result in overestimation of organ doses while using planar imaging. Thus, quantitative SPECT/CT imaging would be the ideal approach for ^{111}In-octreotide scintigraphy-based dose estimation for ^{90}Y-DOTATOC therapy and subsequent response assessment.

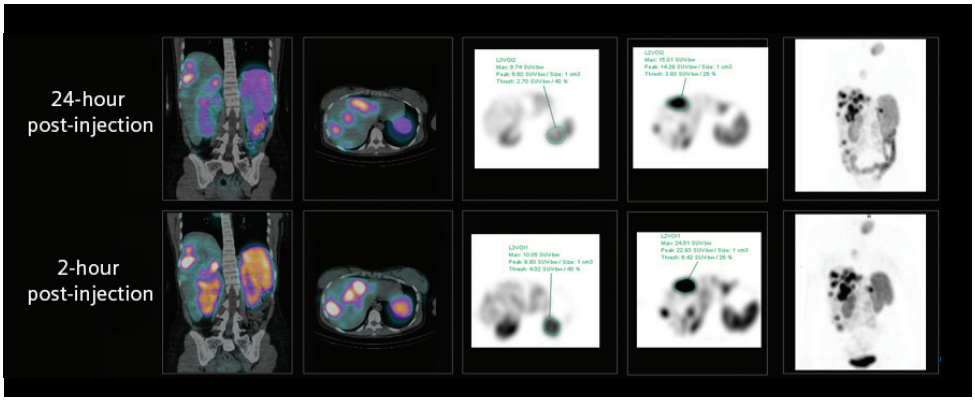

Figure 14: Sequential SPECT/CT studies in a patient with metastatic neuroendocrine tumor performed 2 and 24 hours following administration of 180 MBq of ^{111}In-octreotide. xSPECT Quant demonstrates high SUV_{max} of 24.51 in large liver tumor with slight decrease to SUV_{max} of 15.01 which corresponds to the visual decrease in uptake intensity in the 24-hour image using similar SUV scale. The left kidney shows SUV_{max} of 10.05 at 2 hours and 6.74 at 24 hours, reflecting progressive washout of tracer from renal cortex.

Data courtesy of CHUV, Lausanne, Switzerland.

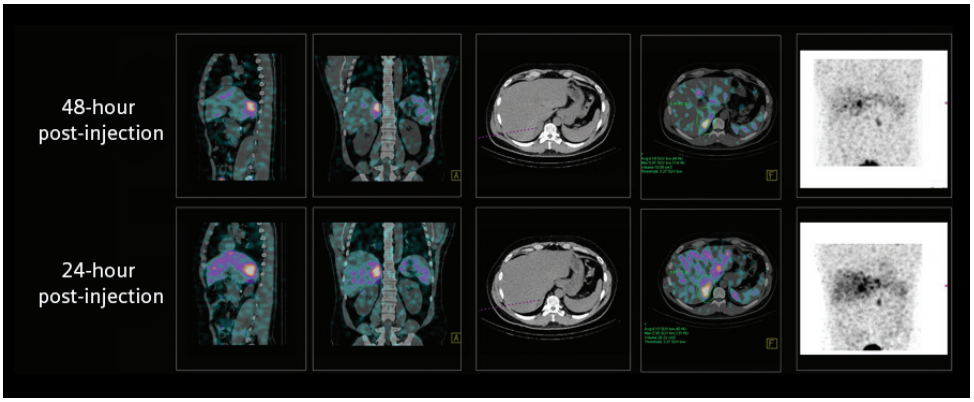

Figure 15: Sequential SPECT/CT images using xSPECT Quant acquired 24 hours and 48 hours after injection of 415 MBq of ^{123}I-MIBG to a patient with metastatic pheochromocytoma. Study shows tracer-avid liver metastases with SUV_{max} of 5.95 in the 24-hour image, which remains unchanged in the study acquired the next day (SUV_{max} of 5.91 in the 48-hour study). The normally functioning left adrenal gland shows similar focal uptake in both studies.

Data courtesy of CHUV, Lausanne, Switzerland.

^{123}I-related applications

^{123}I-MIBG scintigraphy has been a mainstay for diagnosis of neuroblastoma planning ^{131}I-MIBG therapy as well as therapy response evaluation. Quantitative SPECT/CT for absolute tracer concentration and SUV estimation for ^{123}I-MIBG has the potential of improving appropriate patient and dose selection for ^{131}I-MIBG therapy as well as accurate estimation of tumor burden before and after therapy to determine true response and need for further therapy. Semi-quantitative approaches determining tumor to liver count ratio in ^{123}I-MIBG SPECT/CT have shown that the ratio was highest in neuroblastoma than in the ganglioneuroma group and that higher ^{123}I-MIBG uptake and tumor to liver ratio correlates with higher mitotic index related to more aggressive tumors.[26] SUV estimations using quantitative SPECT/CT can potentially improve over ratio analysis for prognostic evaluation in neuroblastoma and impact decision on amount and number of ^{131}I-MIBG therapies, as well as objectively assess therapy response.

Planar ^{123}I-MIBG scans have been semi-quantitatively scored by dividing the body into multiple segments and adding the number of lesions or scoring the uptake intensity and adding them. A higher score reflects higher tumor burden and has been associated with poor outcome after chemotherapy or ^{131}I-MIBG therapy.[27] Using quantitative SPECT/CT, total metabolic tumor volume (MTV) can be determined which potentially would serve as a more robust indicator of total tumor burden and improved prognostic indicator.

Apart from estimation of disease burden and prognostication, ^{123}I-MIBG scintigraphy has also been used to predict radiation dose following ^{131}I-MIBG therapy. Monsieurs et al.[28] performed sequential planar whole-body ^{123}I-MIBG pre-therapy scans immediately and 5 and 24 hours after tracer injection in 38 patients with neuroblastoma or pheochromocytoma. A phantom containing a known activity of ^{123}I was scanned along with the patients for estimation of tissue concentration of ^{123}I-MIBG. Following ^{123}I-MIBG therapy with a mean dose of 5.3 GBq, planar studies were done on days 3, 6, and 10 with simultaneous scanning of phantom with known amount of ^{131}I. Total body dose to the patient was calculated based on a single exponential fit drawn through the time activity curve generated from the sequential planar ^{123}I-MIBG. Patient dose was also calculated by

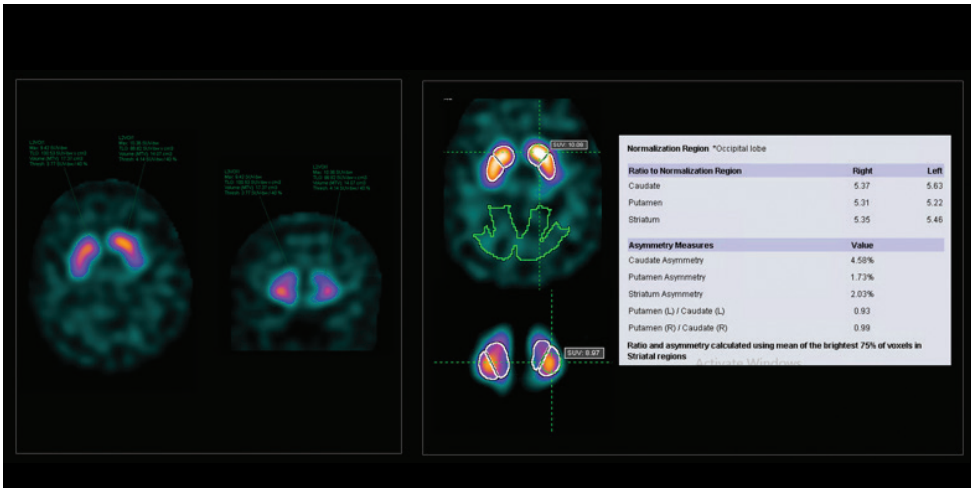

Figure 16: ^{123}I-Ioflupane (DaTscan) SPECT/CT study with xSPECT Quant demonstrating normal striatal uptake in a patient with normal striatal dopaminergic receptor density. Study shows SUV estimation in both striatum with SUV_{max} of 9.42 in the right and 10.38 in the left striatum. Analysis of striatal binding ratio shows right and left SBR or 5.35 and 5.46, respectively, with normal putamen/caudate ratio (0.99-Rt 0.93-Lt). The SUV at the center of the left caudate marked by cursor is 10.08.

Data courtesy of CHUV, Lausanne, Switzerland.

combining time activity curves of ^{123}I-MIBG pre-therapy and ^{131}I-MIBG post-therapy scans and generating a bi-exponential fit from the combined data. The mean total body dose calculated on the basis of a single exponential fit through the data of the ^{123}I-MIBG pre-therapy scans was 0.69 ± 0.38 Gy while the same using a bi-exponential fit using both ^{123}I and ^{131}I-MIBG studies was 0.84 ± 0.51 Gy. Although the calculated dose using ^{123}I-MIBG studies was lower, there was good correlation with that obtained using bi-exponential fit when a correlation factor was used to account for the difference in tracer clearance between pre-therapy and post-therapy scans. This study illustrates the potential of pre-therapy ^{123}I-MIBG scintigraphy to predict dose following ^{131}I-MIBG therapy. Quantitative estimation of ^{123}I-MIBG concentration in tumor and critical organs like bone marrow, kidney, liver, and spleen using sequential SPECT/CT can potentially generate accurate time activity curves to reliably predict tumor and critical organ dose following ^{131}I-MIBG therapy.

Quantification of ^{123}I concentration in ^{123}I-FPCIT (DaTscan) brain SPECT/CT studies may support characterization and classification of Parkinson's disease and related neurodegenerative disorders. SPECT and SPECT/CT studies using DaTscan currently quantify striatal dopamine receptor binding by calculating specific binding ratio (SBR), which is obtained by dividing the striatal uptake by the background uptake. Caudate/putamen ratios and striatal asymmetry is also calculated based on software estimation of caudate and putaminal counts and right and left striatal uptake. Normals databases for DaTscan have been established, which show gender-specific variations as well as age-related decline in SBR.[29] Use of parameters such as SUV to quantify striatal DAT binding would be a novel evaluation approach and correlation of absolute tracer concentration in striatum to clinical criteria may improve characterization of Parkinson's disease, especially in early stages. Use of absolute quantification with DaTscan SPECT/CT may require further normals database creation.

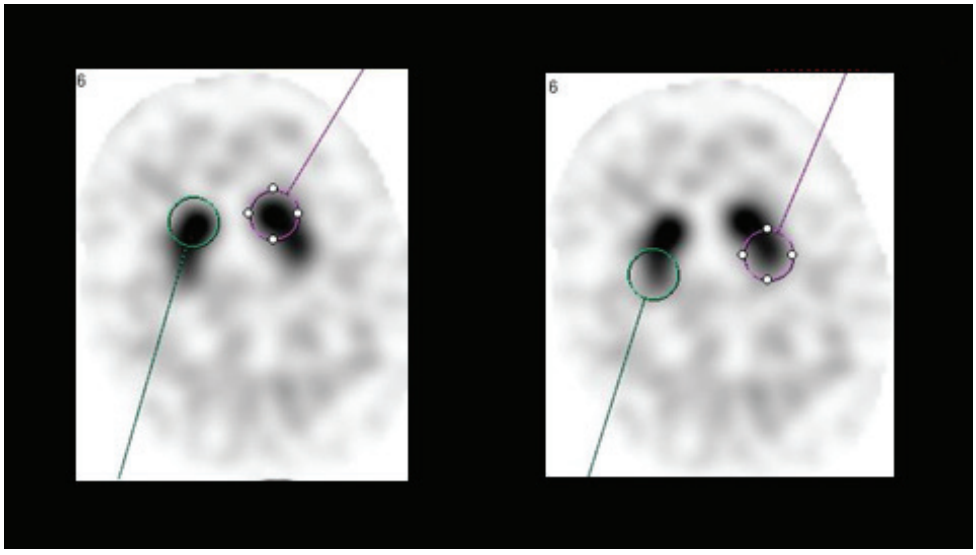

Figure 17: SUV_{max} and SUV_{peak} of caudate and putamen on both sides in the normal patient showing caudate SUV_{max} of 11.37 and putaminal SUV_{max} of 9.84 on the left side, reflecting the left sided putamen to caudate ratio of 0.93.

Data courtesy of CHUV, Lausanne, Switzerland.

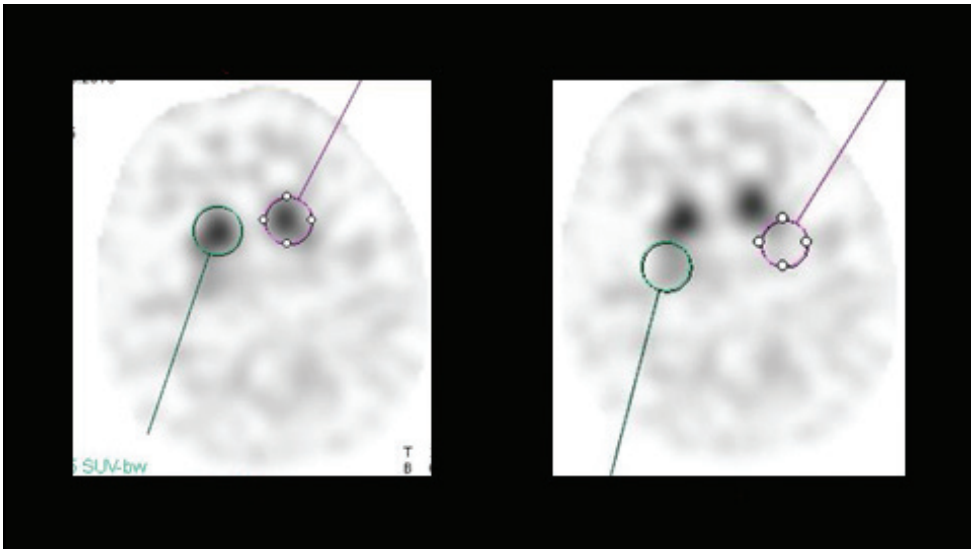

Figure 18: Bilateral caudate and putaminal SUV_{max} and SUV_{peak} values calculated using xSPECT Quant using ^{123}I-Ioflupane (DaTscan) in a patient with Parkinson's disease. Caudate SUV_{max} is 7.75 and Putaminal SUV_{max} is 4.12 on the left side with putamen/caudate ratio of 0.53. This is in sharp contrast to the SUV_{max} and ratio estimations in the normal patient (Figure 17: caudate SUV_{max} of 11.37, putamen SUV_{max} of 9.84, putamen/caudate ratio of 0.93).

Data courtesy of CHUV, Lausanne, Switzerland.

Conclusion

xSPECT technology represents a paradigm shift for the industry. As clinicians try to carefully construct calibration, acquisition, and reconstruction to meet the stringent needs of absolute quantification in SPECT, xSPECT introduces an independent gold standard (3% traceable NIST source) for both the dose calibrator and the imaging system itself. xSPECT incorporates an additive update mechanism, a more accurate model of the image formation physics, a measured LEHR, MELP and LPHR PSF over the entire FOV of the detector at various heights, and the capability to use extra-modal information to enhance nuclear reconstructions.

In summary, as compared to conventional reconstruction techniques which use relative quantification methods, xSPECT Quant not only improves image quality but introduces for the first time in nuclear medicine a standardized approach to produce accurate and reproducible quantitative values across patients, cameras, and sites, that will further support clinical decision-making and help monitor disease response to therapy.

The introduction of xSPECT Quant for absolute quantification of ^{177}Lu, ^{111}In, and ^{123}I is a major step toward implementation and expansion of standardized evidence-based medicine in the realm of radionuclide imaging. Quantitative imaging involving tracers essential to both diagnosis and radionuclide therapy will have a far-reaching impact in the expansion of nuclear medicine into the expanding field of theranostics.

Authors

A. Hans Vija, PhD
Dr. Alexander Hans Vija is the head of the SPECT research team at Siemens Healthineers, Molecular Imaging. He earned his PhD in Physics in 2001, from the University of Washington, Seattle.

Dr. Vija and his team developed technology behind the products: Flash 3D, attenuation correction, enhanced planar processing, IQ•SPECT, xSPECT Quant and xSPECT Bone, and Symbia and Symbia Intevo SPECT/CT systems. He also established, and is conducting worldwide, clinical research collaborations.

He has over 20 publications and holds over 40 US patents and was awarded Siemens AG's "Inventor of the Year" in 2013.

Dr. Carl von Gall, MD
Dr. Carl von Gall is the product manager for *syngo*.via® Oncology applications at Siemens Healthineers, Molecular Imaging. He is a nuclear medicine physician with several years of clinical experience in advanced therapy regimes and imaging, as well as general internal oncology.

Dr. Partha Ghosh, MD
Dr. Partha Ghosh is the clinical marketing advisor for Siemens Healthineers, Molecular Imaging. Dr. Ghosh is a nuclear medicine physician working in the industry for over 15 years with major interest in advanced clinical applications and technological advancements in PET, SPECT, and MRI.

References

[1] D. L. Bailey and K. P. Willowson, "Quantitative SPECT/CT: SPECT joins PET as a quantitative imaging modality," *European Journal of Nuclear Medicine and Molecular Imaging,* vol. 41, pp. S17-S25, 2014.

[2] D. L. Bailey and K. P. Willowson, "An Evidence-Based Review of Quantitative SPECT Imaging and Potential Clinical Applications," Journal of Nuclear Medicine, vol. 54, pp. 83-89, January 1, 2013.

[3] P. Ritt, H. Vija, J. Hornegger, and T. Kuwert, "Absolute quantification in SPECT," *European Journal of Nuclear Medicine and Molecular Imaging,* vol. 38, pp. S69-S77, 2011.

[4] J. Zeintl, A. H. Vija, A. Yahil, J. Hornegger, and T. Kuwert, "Quantitative Accuracy of Clinical ^{99m}Tc SPECT/CT Using Ordered-Subset Expectation Maximization with 3-Dimensional Resolution Recovery, Attenuation, and Scatter Correction," *Journal of Nuclear Medicine,* vol. 51, pp. 921-928, 2010.

[5] J.-M. Beauregard, M. S. Hofman, J. M. Pereira, P. Eu, and R. J. Hicks, "Quantitative ^{177}Lu SPECT (QSPECT) Imaging Using a Commercially Available SPECT/CT System," *Cancer Imaging,* vol. 11, pp. 56-66, 2011.

[6] M. Elschot, J. F. W. Nijsen, M. G. E. H. Lam, M. L. J. Smits, J. F. Prince, M. A. Viergever, M. A. A. J. van den Bosch, B. A. Zonnenberg, and H. W. A. M. de jong, "^{99m}Tc-MAA overestimates the absorbed dose to the lungs in radioembolization: a quantitative evaluation in patients treated with ^{166}Ho-microspheres," *European Journal of Nuclear Medicine and Molecular Imaging,* vol. 41, pp. 1965-1975, 2014.

[7] R. de Nijs, V. Lagerburg, T. L. Klausen, and S. Holm, "Improving quantitative dosimetry in ^{177}Lu-DOTATATE SPECT by energy window-based scatter corrections," Nuclear Medicine Communications, vol. 35, pp. 522-533, 2014.

[8] G. El Fakhri, M. F. Kijewski, M. S. Albert, K. A. Johnson, and S. C. Moore, "Quantitative SPECT leads to improved performance in discrimination tasks related to prodromal Alzheimer's disease," *Journal of Nuclear Medicine,* vol. 45, p. 2026, 2004.

[9] D. E. Bergeron, J. T. Cessna, D. B. Golas, R. K. Young, and B. E. Zimmerman, "Dose calibrator manufacturer-dependent bias in assays of ^{123}I," Applied Radiation and isotopes, vol. 90, pp. 79-83, 2014.

[10] A. H. Vija, "Introduction to xSPECT Technology: Evolving Multi-modal SPECT to Become Context-based and Quantitative," Siemens Medical Solutions USA, Inc., *Molecular Imaging*, White Paper 2013.

[11] K. J. Mighell, "Parameter Estimation in Astronomy with Poisson-Distributed Data. I. The Chi-Square-Lambda Statistic," *The Astrophysical Journal,* vol. 518, pp. 380-393, 1999.

[12] Cachovan M, Vija AH, Hornegger J., Kuwert T., "Quantification of ^{99m}Tc-DPD Concentration in the Lumbar Spine SPECT/CT," *European Journal of Nuclear Medicine and Molecular Imaging.* 2013;3:1-8.

[13] Kjaer et al, "Use of radioactive substances in diagnosis and treatment of neuro-endocrine tumors," *Scand J Gastroenterol*, 2015; 50(6): 740-747.

[14] Bodei et al, "Long-term tolerability of PRRT in 807 patients with neuroendocrine tumours: the value and limitations of clinical factors," *Eur J Nucl Med Mol Imaging* 2015;42:-19.

[15] Kwekkeboom et al, "Treatment With the Radiolabeled Somatostatin Analog [^{177}Lu-DOTA0, Tyr3] Octreotate: Toxicity, Efficacy, and Survival," *Journal of Clinical Oncology* 26 2124-2130.

[16] Garkavij et al, "^{177}Lu (DOTA0,Tyr3) octreotate therapy in patients with disseminated neuroendocrine tumor: Analysis of dosimetry with impact on future therapeutic strategy." *Cancer* Vol 116, Supplement S4, February 2010 Pages 1084-1092.

[17] Valkema et al, "Long-Term Follow-Up of Renal Function After Peptide Receptor Radiation Therapy with ^{90}Y-DOTA0, Tyr3-Octreotide and ^{177}Lu-DOTA0, Tyr3-Octreotate," *J Nucl Med.* 2005;46 Suppl 1:83S-91S.

[18] Bergsma et al, "Nephrotoxicity after PRRT with ^{177}Lu-DOTA-octreotate," Eur J Nucl Med Mol Imaging (2016) 43:1802–1811.

[19] Beauregard et al, "The tumour sink effect on the biodistribution of ^{68}Ga-DOTA-octreotate: implications for peptide receptor radionuclide therapy," *Eur J Nucl Med Mol Imaging* (2012) 39:50-56.

[20] Konijnenberg et al, "Radiation Dose Distribution in Human Kidneys by Octreotides in Peptide Receptor Radionuclide Therapy," *J Nucl Med.* 2007;48:134-142.

[21] Ilan et al, "Dose Response of Pancreatic Neuroendocrine Tumors Treated with Peptide Receptor Radionuclide Therapy Using ^{177}Lu-DOTATATE," *J Nucl Med* 2015; 56:177-182.

[22] Sandstrom et al, "Individualized Dosimetry of Kidney and Bone Marrow in Patients Undergoing ^{177}Lu-DOTA-Octreotate Treatment," *J Nucl Med* 2013; 54:33-41.

[23] Bailey et al, "*In Vivo* Measurement and Characterization of a Novel Formulation of [177Lu]-DOTA-Octreotate," Asia Oceania *J Nucl Med Biol.* 2016; 4(1):30-37.

[24] Rowe et al, "Repeatability of Radiotracer Uptake in Normal Abdominal Organs with ^{111}In-Pentetreotide Quantitative SPECT/CT," *J Nucl Med.* 2015 July; 56(7): 985-988.

[25] Helisch et al, "Pre-therapeutic dosimetry and biodistribution of ^{86}Y-DOTA-Phe1-Tyr3-octreotide versus ^{111}In-pentetreotide in patients with advanced neuroendocrine tumours," *Eur J Nucl Med Mol Imaging* (2004) 31:1386-1392.

[26] Fendler et al, "High ^{123}I-MIBG uptake in neuroblastic tumours indicates unfavourable histopathology," *Eur J Nucl Med Mol Imaging* 2013; 40:1701-1710.

[27] Matthay et al, "Criteria for evaluation of disease extent by ^{123}I-metaiodobenzyl-guanidine scans in neuroblastoma: a report for the International Neuro-blastoma Risk Group (INRG) Task Force," *British Journal of Cancer* (2010) 102, 1319-1326.

[28] Monsieurs et al, "Patient dosimetry for ^{131}I-MIBG therapy for neuroendocrine tumours based on ^{123}I-MIBG scans," *Eur J Nucl Med Mol Imaging* (2002) 29:1581-1587.

[29] Varrone et al, "European multicentre database of healthy controls for [123I] FP-CIT SPECT (ENC-DAT): age-related effects, gender differences and evaluation of different methods of analysis," *Eur J Nucl Med Mol Imaging* (2013) 40:213-227.

Trademarks and service marks used in this material are property of Siemens Healthcare GmbH. All other company, brand, product and service names may be trademarks or registered trademarks of their respective holders.

All comparative claims derived from competitive data at the time of printing. Data on file. Siemens reserves the right to modify the design and specifications contained herein without prior notice. As is generally true for technical specifications, the data contained herein varies within defined tolerances. Some configurations are optional. Product performance depends on the choice of system configuration.

Please contact your local Siemens sales representative for the most current information or contact one of the addresses listed below. Note: Original images always lose a certain amount of detail when reproduced.

"Siemens Healthineers" is considered a brand name. Its use is not intended to represent the legal entity to which this product is registered. Please contact your local Siemens organization for further details.

All photographs © 2018 Siemens Healthcare GmbH. All rights reserved.

[a] We also provide an alternate calibration protocol that does not offer the advantage of standardization, but can be used as a fall back in case the CSS is not available.

xSPECT Quant and Broad Quantification are not commercially available in some countries. Due to regulatory reasons, their future availability cannot be guaranteed. Please contact your local Siemens organization for further details.

^{99m}Tc antigranulocyte antibody referenced herein is not currently recognized by the US FDA as being safe and effective, and Siemens does not make any claims regarding its use.

^{90}Y-DOTATOC is not commercially available in some countries, including the US. ^{90}Y-DOTATOC is not currently recognized by the US FDA as being safe and effective, and Siemens does not make any claims regarding its use. Due to regulatory reasons, its future availability cannot be guaranteed. Please contact your local Siemens organization for further details.

Siemens Healthineers Headquarters
Siemens Healthcare GmbH
Henkestr. 127
91052 Erlangen, Germany
Phone: +49 9131 84 0
siemens.com/healthineers

Published by
Siemens Medical Solutions USA, Inc.
40 Liberty Boulevard
Malvern, PA 19355-9998
USA
Phone: +1 888 826-9702
siemens-healthineers.com

Global Business Line
Siemens Medical Solutions USA, Inc.
Molecular Imaging
2501 North Barrington Road
Hoffman Estates, IL 60192
USA
Phone: +1 847 304-7700
siemens.com/mi

Order No. A91MI-10473-T1-7600 | Printed in USA | All rights reserved | MI-3610.TM.JV.TW.1500 | © Siemens Healthcare GmbH, 01.2018